

Weakly nonlinear ion acoustic excitations in a relativistic model for dense quantum plasma

E. E. Behery,^{1,2,*} F. Haas,^{3,†} and I. Kourakis^{2,‡}

¹*Department of Physics, Faculty of Science,
Damietta University, New Damietta, P.O. 34517, Egypt*

²*Centre for Plasma Physics, Department of Physics and Astronomy,
Queen's University Belfast, Belfast BT7 1NN, Northern Ireland, United Kingdom*

³*Instituto de Física, Universidade Federal do Rio Grande do Sul,
Av. Bento Gonçalves 9500, CEP 91501-970, Porto Alegre, RS, Brazil*

(Dated: February 4, 2016)

Abstract

The dynamics of linear and nonlinear ionic-scale electrostatic excitations propagating in a magnetized relativistic quantum plasma is studied. A quantum-hydrodynamic model is adopted and degenerate statistics for the electrons is taken into account. The dispersion properties of linear ion acoustic waves (IAWs) are examined in detail. A modified characteristic charge screening length and “sound speed” are introduced, for relativistic quantum plasmas. By employing the reductive perturbation technique, a Zakharov-Kuznetsov (ZK) type equation is derived. Using the small $-k$ expansion method, the stability profile of weakly nonlinear slightly supersonic electrostatic pulses is also discussed. The effect of electron degeneracy on the basic characteristics of electrostatic excitations is investigated. The entire analysis is valid in a three-dimensional (3D) as well as in two-dimensional (2D) geometry. A brief discussion of possible applications in laboratory and space plasmas is included.

I. INTRODUCTION

Electron degeneracy in dense quantum plasmas has recently gained increasing interest, due to its relevance in a wide range of plasmas in astrophysics, and also in modern technological applications. Dense quantum plasmas are found in ultraintense laser beam-solid matter interaction experiments [1], in which the plasmon frequency is measurably shifted due to quantum effects [2, 3]. Quantum plasmas are relevant in femto-second pump-probe spectroscopy connected to the collective dynamics of degenerate electrons in metallic nanostructures and thin films [4], in the physics of quantum diodes [5], nanophotonics and nanowires [6], nanoplasmonics [7], high-gain quantum free-electron lasers [8], quantum wells and piezomagnetic quantum dots [9]. Degenerate plasmas may also exist in dense astrophysical objects, e.g. in the core of giant planets [10] and in the crust of white dwarfs, brown dwarfs, neutron stars, and magnetars [11, 12].

In a degenerate plasma, the electron number density is extremely high and the temperature is very low. When the de Broglie wavelength of electrons (which is the spatial extension of the wave function due to the quantum uncertainty principle) can be comparable to, or larger than, the average inter-electron distance $d = n_e^{-1/3}$, quantum effects become significant and can not be ignored. Electrons can more easily reach the quantum regime than ions because of their smaller mass; at room temperature electrons begin to behave quantum mechanically at number density of about 10^{20} cm^{-3} , while the electron density for metals is normally larger than 10^{22} cm^{-3} , giving rise to electron Fermi temperature of order 10^4 K , to be considered within the quantum regime. The continuous motion of an electron in degenerate plasma around its position exerts a pressure on the surrounding plasma; this pressure is referred to as the electron degeneracy pressure P_e . An expression for the degeneracy pressure was employed by Chandrasekhar [13, 14] to estimate the critical mass limit of white dwarfs. Recently, Shukla and Eliasson [15, 16] discussed theoretically the nonlinear aspects and collective interactions for degenerate plasmas. Later, Haas and Kourakis [17] used the one-dimensional version of the electron pressure equation, expressed by Chandrasekhar [13, 14], to study the evolution of hydrodynamic Langmuir waves in fully degenerate relativistic plasma. McKerr *et al.* adopted the same fluid model to investigate the occurrence of modulated envelope structures within a (1D) nonlinear Schrödinger (NLS) framework [18].

Interestingly, the existence of acoustic-type modes has been proposed in white dwarf stars [19, 20], where ions might provide the inertia while the electron degeneracy pressure may provide the restoring force. Although such modes have been argued to exist [21], these haven't been observed to date [20]. The possibility for the occurrence of acoustic waves was also suggested in relevance with extreme events such as supernova explosions [19, 22]. Various theoretical investigations have been proposed, predicting excitations which are yet to be detected [23–26].

The propagation of small amplitude nonlinear excitations, in the form of electrostatic pulses, in a multidimensional (2D or 3D) plasma geometry is known to be governed by the Zakharov-Kuznetsov (ZK) equation [27], which is a generic paradigm for solitary waves in dispersive media [28]. The ZK equation can be viewed as a canonical multidimensional extension of the Korteweg-de Vries (KdV) equation [29]. Zakharov and Kuznetsov [27] used this equation to study the behavior of weakly nonlinear ion acoustic waves (IAWs) in plasma comprising cold ions and hot isothermal electrons in the presence of a uniform magnetic field. Frycz and Infeld [30] investigated the instability of small amplitude nonlinear waves by using the solutions of the ZK equation. Later, Allen and Rowlands [31, 32] investigated the stability profile of solutions of the ZK equation via the k - expansion perturbation method, based on the Floquet theorem. The small- k expansion perturbation method [31, 32] has also been employed to study the instability of nonlinear waves obliquely propagating in magnetized plasmas [33–35].

In this article, we have considered a three-dimensional (3D) fluid model for ion acoustic excitations in a degenerate relativistic plasma immersed in an external static magnetic field. The electron pressure is assumed to be described by a Chandrasekhar type equation of state [13, 14]. At a first step, we have carried out a Fourier-type linear analysis, to identify linear modes occurring in this model. A modified ion-acoustic wave was thus shown to exist, alongside a Langmuir-like “optical” mode, characterized by a frequency cutoff at the origin. Proceeding the analysis by anticipating stationary-profile solitary structures, we have adopted a small-amplitude nonlinear multi-scale (reductive perturbation) theory, in search of an evolution equation for the amplitude of an electrostatic perturbation. The analysis shows that these structures may be unstable to external perturbations, which is arguably due to the effect of bilateral perturbations, in contrast with the one-dimensional case [31, 32].

This paper is organized in the following manner. In Section II, we introduce a relativistic

plasma fluid model for low-frequency (ionic scale) electrostatic waves. A linear analysis is carried out, and the existence and dispersion characteristics of linear modes are discussed in Section IV. A nonlinear perturbation technique is employed in Section V, where we show that the electrostatic potential is governed by a Zakharov-Kuznetsov equation. The characteristic properties of solitary waves occurring as exact solution of the model are examined in Section VI. The stability of the localized solutions is investigated via an adequate multiscale (small- k expansion) methodology in Section VII. Finally, we discuss our results in the concluding Section VIII.

II. THE MODEL

Let us consider the propagation of ion acoustic (IA) excitations in a degenerate relativistic plasma, in the presence of an external static magnetic field aligned to the z -direction: $\mathbf{B} = B_0 \hat{z}$ (where B_0 denotes the magnetic field strength and \hat{z} is the unit vector along z). We shall adopt the relativistic plasma fluid model introduced in Ref. 18, extending it to a multidimensional geometry, in the form:

$$\frac{\partial}{\partial t} (\gamma_i n_i) + \nabla \cdot (\gamma_i n_i \mathbf{u}_i) = 0, \quad (1)$$

$$\frac{\partial}{\partial t} (\gamma_e n_e) + \nabla \cdot (\gamma_e n_e \mathbf{u}_e) = 0, \quad (2)$$

$$\frac{\partial}{\partial t} (\gamma_i \mathbf{u}_i) + (\mathbf{u}_i \cdot \nabla) (\gamma_i \mathbf{u}_i) = \frac{-e z_i}{m_i} \nabla \phi + \frac{e z_i B_0}{m_i} (\mathbf{u}_i \times \hat{z}), \quad (3)$$

$$0 = e \nabla \phi - e B_0 (\mathbf{u}_e \times \hat{z}) - \frac{m_e c^2 \gamma_e}{P_e + \rho_e} \left(\nabla + \frac{\mathbf{u}_e}{c^2} \frac{\partial}{\partial t} \right) P_e, \quad (4)$$

$$\nabla^2 \phi = \frac{e}{\epsilon_0} (\gamma_e n_e - \gamma_i z_i n_i), \quad (5)$$

where n_e and n_i and denote the electron and ion fluid number densities, respectively, \mathbf{u}_e and \mathbf{u}_i are the corresponding fluid velocities and the electron mass (m_e), ion mass (m_i), electron charge (e , in absolute value), ionic charge ($+z_i e$) and light speed (c) carry their usual notation. The latter system has been expressed in SI units.

The electron pressure P_e is given by

$$P_e = \frac{m^4 c^5}{24 \pi^2 \hbar^3} \left[\alpha (2\alpha^2 - 3) (\alpha^2 + 1)^{1/2} + 3 \sinh^{-1} \alpha \right], \quad (6)$$

where $\hbar = h/2\pi$ is the reduced Planck constant. Furthermore [18],

$$P_e + \rho_e = n_e m_e c^2 \sqrt{\alpha^2 + 1}, \quad (7)$$

where ρ_e is the electron fluid internal energy density. We have defined the parameter

$$\alpha = \frac{p_{Fe}}{m_e c} = \frac{\hbar}{m_e c} (3\pi^2 n_e)^{1/3}. \quad (8)$$

Considering the equilibrium state, we shall also define

$$\alpha_0 = \frac{\hbar}{m_e c} (3\pi^2 n_{e0})^{1/3}, \quad \text{hence} \quad \alpha = \alpha_0 \left(\frac{n_e}{n_{e0}} \right)^{1/3}.$$

Charge neutrality condition at equilibrium imposes $n_{e0} = z_i n_{i0}$.

It should be noted, for rigor, that an additional quantum term, namely the so-called Bohm potential, in account of quantum diffraction, could have been added to the momentum equations. Such a contribution, however, would be comparable to the Fermi pressure only for extremely small wavelengths of the order of the mean inter-particle distance [36], and will therefore be omitted in this study.

III. SCALING AND DIMENSIONLESS MODEL

We shall normalize Eqs. (1-5), upon setting, formally $\nabla \rightarrow L_0^{-1} \tilde{\nabla}$, $t \rightarrow T_0 \tilde{t}$, $\mathbf{u}_i \rightarrow V_0 \tilde{\mathbf{u}}_i$, $\mathbf{u}_e \rightarrow V_0 \tilde{\mathbf{u}}_e$ and $\phi \rightarrow \varphi_0 \tilde{\phi}$, where the tilde'd quantities are dimensionless. Once the transformation has been carried out, leading to the system of Eqs. (9)-(13) below, the tilde will be omitted in the following, for simplicity. The scaling quantities adopted above were chosen appropriately as:

$$L_0 = \left(\frac{\epsilon_0 E_{Fe}}{e^2 z_i^2 n_{i0}} \right)^{1/2}, \quad V_0 = \frac{L_0}{T_0} = \left(\frac{E_{Fe}}{m_i} \right)^{1/2},$$

$$T_0 = \omega_{pi}^{-1} = \left(\frac{\epsilon_0 m_i}{e^2 z_i^2 n_{i0}} \right)^{1/2} \quad \text{and} \quad \varphi_0 = \frac{E_{Fe}}{e z_i}.$$

The electron Fermi energy E_{Fe} in the relativistic regime reads

$$E_{Fe} = \sqrt{p_{Fe}^2 c^2 + m_e^2 c^4} - m_e c^2.$$

Combining with Eqs. (1)-(8), we obtain the following set of normalized (dimensionless)

equations:

$$\frac{\partial}{\partial t} (\gamma_i n_i) + \nabla \cdot (\gamma_i n_i \mathbf{u}_i) = 0, \quad (9)$$

$$\frac{\partial}{\partial t} (\gamma_e n_e) + \nabla \cdot (\gamma_e n_e \mathbf{u}_e) = 0, \quad (10)$$

$$\frac{\partial}{\partial t} (\gamma_i \mathbf{u}_i) + (\mathbf{u}_i \cdot \nabla) (\gamma_i \mathbf{u}_i) = -\nabla \phi + \Omega (\mathbf{u}_i \times \hat{z}), \quad (11)$$

$$0 = \nabla \phi - \Omega (\mathbf{u}_e \times \hat{z}) - \frac{\beta \alpha_0^2 \gamma_e n_e^{-1/3}}{\alpha_0^2 n_e^{2/3} + 1} \left(\nabla + \delta \mathbf{u}_e \frac{\partial}{\partial t} \right) n_e, \quad (12)$$

$$\nabla^2 \phi = \gamma_e n_e - \gamma_i n_i, \quad (13)$$

where we have defined the quantities

$$\begin{aligned} \Omega &= \frac{e z_i B_0 T_0}{m_i} = \frac{\omega_{ci}}{\omega_{pi}}, & \beta &= \frac{m_e c^2}{3e\phi_0} = \frac{m_e c^2 z_i}{3E_{Fe}}, \\ \text{and} \quad \delta &= \frac{V_0^2}{c^2} = \frac{E_{Fe}}{m_i c^2}. \end{aligned} \quad (14)$$

The above system of equations forms the basis of the analysis that follows. All quantities are henceforth to be considered as dimensionless, unless otherwise stated.

IV. LINEAR ANALYSIS

Let us consider small amplitude harmonic excitations, by assuming that all of the state variables vary as

$$G = G_0 + G_1 e^{i(\mathbf{k} \cdot \mathbf{r} - \omega t)},$$

where $G = [n_i, n_e, \mathbf{u}_i, \mathbf{u}_e, \phi]$ is the state vector. The reference state and the corresponding (small) perturbation are expressed as $G_0 = [1, 1, 0, 0, 0]$ and $G_1 = [n_{i1}, n_{e1}, \mathbf{u}_{i1}, \mathbf{u}_{e1}, \phi_1]$ (the notation adopted here is self-explanatory). A lengthy set of linear equations is thus obtained, in terms of the in terms of the normalized frequency ω and the wavenumber \mathbf{k} (components). A tedious but perfectly straightforward calculation leads to the dispersion relation

$$\omega^4 - [\omega_0^2(k) + \Omega^2] \omega^2 + \frac{k_{\parallel}^2}{k^2 + F^{-1}} \Omega^2 = 0, \quad (15)$$

where we have defined the quantity $F = \frac{\beta \alpha_0^2}{\alpha_0^2 + 1}$. The modulus of the wavevector is expressed in the usual way as $k^2 = k_x^2 + k_y^2 + k_z^2 \equiv k_{\parallel}^2 + k_{\perp}^2$. The function

$$\omega_0^2(k) = \frac{k^2}{k^2 + F^{-1}}, \quad (16)$$

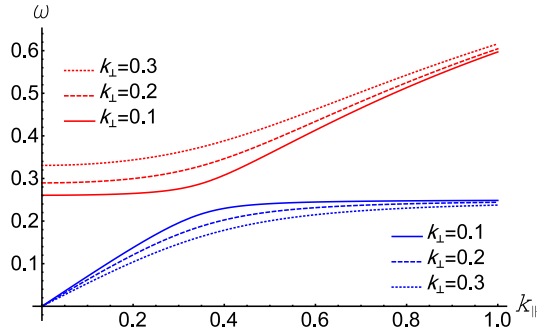


FIG. 1: (Color online) The angular frequency ω (scaled by ω_{pi}) is depicted versus the parallel component of the wavenumber $k_{||}$ (scaled by L_0^{-1}). Here, the lower curves (blue color) and the upper curve(s) (red color) represent the lower (acoustic) and upper (Langmuir-like) mode, ω_- and ω_+ , respectively. We have taken $n_{e0} = 1 \times 10^{35} \text{ m}^{-3}$, i.e. $\alpha_0 = 0.55$, $E_{Fe} = 73.4 \text{ KeV}$, $\Omega(= \omega_{ci}/\omega_{pi}) = 0.25$.

represents the frequency (square) of linear IAWs in an unmagnetized plasma (to see this, set $\Omega = 0$ in the latter dispersion relation, to obtain $\omega = \omega_0(k)$).

The solution of the dispersion relation (15) reads

$$\omega_{\pm}^2 = \frac{1}{2} [\omega_0^2(k) + \Omega^2] \times \left[1 \pm \sqrt{1 - \frac{4k_{||}^2}{(k^2 + F^{-1}) [\omega_0^2(k) + \Omega^2]^2}} \right]. \quad (17)$$

We note the existence of two modes, namely a lower (slow) mode, ω_- , and an upper (fast) mode, ω_+ . These represent, respectively, an acoustic mode and a Langmuir-like mode, the latter featuring a cutoff (gap) frequency in the infinite wavelength limit. The two dispersion curves are depicted in Figures 1-5. (Clearly, the analogy with Langmuir waves is only structural here: this mode is sustained by the ion inertia too, instead of the electron inertia -here neglected- which would sustain electron plasma-Langmuir waves, properly speaking.)

A. Parallel propagation

Let us consider the case $k = k_{||}$ (viz., $k_{\perp} = 0$). The dispersion relation (15) reduces to

$$\omega^4 - [\omega_0^2(k_{||}) + \Omega^2] \omega^2 + \omega_0^2(k_{||}) \Omega^2 = 0, \quad (18)$$

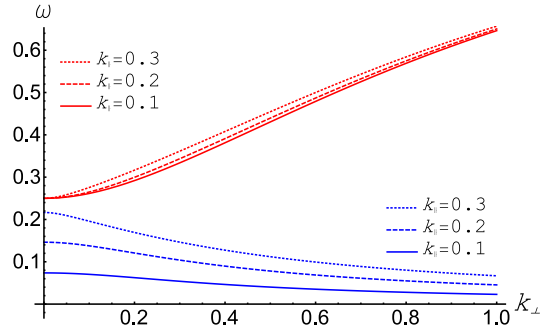


FIG. 2: (Color online) The angular frequency ω (scaled by ω_{pi}) is depicted versus the perpendicular component of the wavenumber k_{\perp} (scaled by L_0^{-1}). Here, the lower curves (blue color) and the upper curves (red color) represent the lower and upper mode, ω_- and ω_+ , respectively. We have taken $n_{e0} = 1 \times 10^{35} \text{ m}^{-3}$, i.e. $\alpha_0 = 0.55$, $E_{Fe} = 73.4 \text{ KeV}$, $\Omega(= \omega_{ci}/\omega_{pi}) = 0.25$.

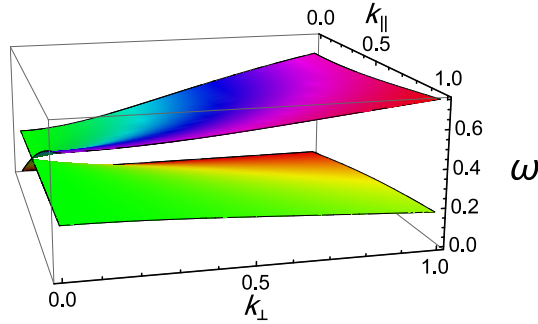


FIG. 3: (Color online) Three-dimensional plot of the lower (acoustic) and upper (Langmuir-like) mode: the angular frequency ω (scaled by ω_{pi}) is depicted versus both parallel and perpendicular components of the wavenumber (k_{\parallel} and k_{\perp} , both scaled by L_0^{-1}). We have taken $n_{e0} = 1 \times 10^{35} \text{ m}^{-3}$, i.e. $\alpha_0 = 0.55$, $E_{Fe} = 73.4 \text{ KeV}$, $\Omega(= \omega_{ci}/\omega_{pi}) = 0.25$.

whose solution, say $\omega = \omega_{\parallel}$, is given by

$$\omega_{\parallel}^2 = \omega_0^2(k_{\parallel}) = \frac{k_{\parallel}^2}{k_{\parallel}^2 + F^{-1}}. \quad (19)$$

Here, we have overlooked a trivial non-propagating solution $\omega = \Omega$. Noting the limits

$$\lim_{k_{\parallel} \rightarrow 0, k_{\perp} \rightarrow 0} \omega_{\parallel} = 0, \quad (20)$$

$$\text{and } \lim_{k_{\parallel} \rightarrow 0} \left(\frac{\omega_{\parallel}}{k_{\parallel}} \right) = \sqrt{F} = \sqrt{\frac{\beta \alpha_0^2}{\alpha_0^2 + 1}}, \quad (21)$$

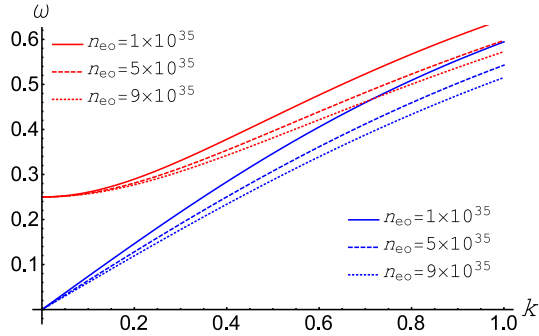


FIG. 4: (Color online) The parallel mode (in blue color) and the perpendicular mode (in red color) (angular frequency ω scaled by ω_{pi}) are depicted versus the wavenumber k (scaled by L_0^{-1}) for different n_{e0} values, taking $\Omega(= \omega_{ci}/\omega_{pi}) = 0.25$.

we deduce that the parallel solution is a propagating acoustic mode and \sqrt{F} is physically to be interpreted as the phase speed of this mode. This is essentially the true “sound speed” in this plasma configuration, taking into account relativistic and degeneracy effects.

B. Perpendicular propagation

Let us now consider the case $k = k_{\perp}$ (i.e., $k_{\parallel} = 0$), in account of propagation in the transverse direction, with respect to the ambient magnetic field (direction). The frequency of transverse modes, say, $\omega = \omega_{\perp}$, is given by the dispersion relation (15) which now reduces to

$$\omega_{\perp}^4 - [\omega_{\perp 0}^2 + \Omega^2] \omega_{\perp}^2 = 0. \quad (22)$$

Hence, the perpendicular frequency can be obtained as

$$\omega_{\perp}^2 = \omega_0^2(k_{\perp}) + \Omega^2, \quad (23)$$

$$\omega_0^2(k_{\perp}) = \frac{k_{\perp}^2}{k_{\perp}^2 + F^{-1}}. \quad (24)$$

Equation (23) shows that the perpendicular mode has a nonzero value Ω^2 at $k_{\perp} \rightarrow 0$. The parallel and perpendicular modes are depicted in Figures 4 and 5.

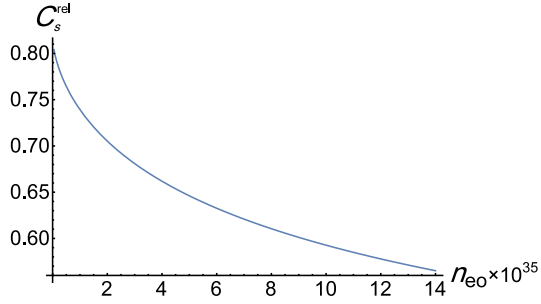


FIG. 5: (Color online) The characteristic “sound speed” C_s^{rel} (scaled by V_0) is depicted versus n_{e0} (in m^{-3}).

C. The unmagnetized limit

In the vanishing magnetic field limit, i.e. upon setting $\Omega = 0$, one obtains

$$\begin{aligned}\omega_-^2 &= 0, \\ \omega_+^2 &= \omega_0^2(k) = \frac{k^2}{k^2 + F^{-1}}.\end{aligned}\tag{25}$$

Equation (25) represents the linear dispersion relation of IAWs in an unmagnetized plasma. As physically expected, the latter dispersion relation coincides with the analogous expression for parallel propagation, since the Lorentz force disappears in the latter case.

D. Asymptotic behavior

For large values of k_{\parallel} , the solution (17) of the dispersion relation (15) behaves as

$$\begin{aligned}\lim_{k_{\parallel} \rightarrow \infty} (\omega_-^2) &= \Omega^2, \\ \lim_{k_{\parallel} \rightarrow \infty} (\omega_+^2) &= 1.\end{aligned}\tag{26}$$

In an analogous way, for large values of k_{\perp} , one obtains

$$\begin{aligned}\lim_{k_{\perp} \rightarrow \infty} (\omega_-^2) &= 0, \\ \lim_{k_{\perp} \rightarrow \infty} (\omega_+^2) &= \Omega^2 + 1.\end{aligned}\tag{27}$$

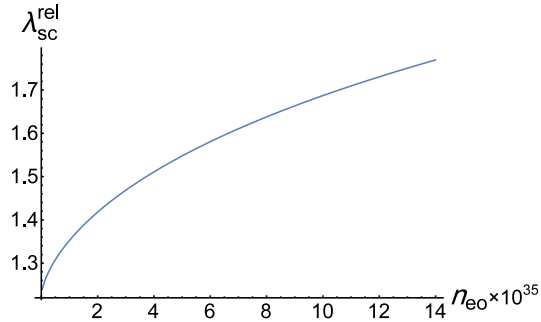


FIG. 6: (Color online) The characteristic charge screening length λ_{sc}^{rel} (scaled by L_0) is depicted versus n_{e0} (in m^{-3}).

E. Relativistic screening mechanism

The cases considered above indicate that the functional form $\omega_0^2(k)$ is an essential characteristic of the wave dispersion. We can rewrite $\omega_0^2(k)$ as

$$\omega_0^2(k) = \frac{k^2}{k^2 + (\lambda_{sc}^{rel})^{-2}}, \quad (28)$$

where λ_{sc}^{rel} is the characteristic charge screening length (here normalized by L_0), in the relativistic regime:

$$\lambda_{sc}^{rel} = F^{-1/2} L_0 = \left(\frac{\beta \alpha_0^2}{\alpha_0^2 + 1} \right)^{-1/2} \left(\frac{\epsilon_0 E_{Fe}}{e^2 z_i^2 n_{io}} \right)^{1/2} \quad (29)$$

λ_{sc}^{rel} is analogous to the classical Debye radius λ_D , here modified in account of relativistic effects. Accordingly, the (modified) “true” sound speed in the plasma C_s^{rel} , taking into account the relativistic correction, reads

$$C_s^{rel} = F^{1/2} V_0 = \left(\frac{\beta \alpha_0^2}{\alpha_0^2 + 1} \right)^{1/2} \left(\frac{E_{Fe}}{m_i} \right)^{1/2}. \quad (30)$$

In the latter two expressions, we have recovered dimensions, for clarity. Figures 5 and 6 indicate the dependence of C_s^{rel} and λ_{sc}^{rel} on n_{e0} . It is clear that $C_s^{rel}(\lambda_{sc}^{rel})$ decreases (increases) as n_{e0} increases.

V. NONLINEAR ANALYSIS

In order to study weak-amplitude superacoustic electrostatic excitations, we may employ the reductive perturbation method of Taniuti and coworkers [37]. A set of stretched

coordinates are introduced as

$$X = \epsilon^{1/2}x, \quad Y = \epsilon^{1/2}y, \quad Z = \epsilon^{1/2}(z - \lambda t), \quad T = \epsilon^{3/2}t,$$

accounting for propagation along the z axis at a speed λ (which is to be defined later by compatibility requirements). The *ad hoc* (real) parameter ϵ is assumed to be small, i.e. $\epsilon \ll 1$. The plasma state variables are expanded near their equilibrium values as

$$\begin{aligned} n_j &= 1 + \epsilon n_{j1} + \epsilon^2 n_{j2} + \dots, \\ u_{jx} &= \epsilon^{3/2} u_{jx1} + \epsilon^2 u_{jx2} + \dots, \\ u_{jy} &= \epsilon^{3/2} u_{jy1} + \epsilon^2 u_{jy2} + \dots, \\ u_{jz} &= \epsilon u_{jz1} + \epsilon^2 u_{jz2} + \dots, \\ \phi &= \epsilon \phi_1 + \epsilon^2 \phi_2 + \dots, \end{aligned} \tag{31}$$

where the subscript j stands for either e (for electrons) or i (for ions).

We proceed by combining the above analytical expansions and the stretched coordinates into Eqs. (9 – 13), and then collecting terms of the same powers of ϵ . At the lowest order, we obtain

$$\begin{aligned} n_{i1} &= \frac{\phi_1}{\lambda^2}, & n_{e1} &= \frac{(\alpha_0^2 + 1)\phi_1}{\beta\alpha_0^2}, \\ u_{iz1} &= \frac{\phi_1}{\lambda}, & u_{ez1} &= \frac{\lambda(\alpha_0^2 + 1)\phi_1}{\beta\alpha_0^2}. \end{aligned} \tag{32}$$

A compatibility condition is imposed, in the form

$$\lambda^2 = \frac{\beta\alpha_0^2}{\alpha_0^2 + 1}, \tag{33}$$

which leads, as a consequence, to $u_{iz1} = u_{ez1}$; cf. Eq.(32).

Now, equating the coefficients of the second higher order of ϵ gives rise to the following set of equations

$$\begin{aligned} \lambda \frac{\partial n_{i2}}{\partial Z} - \frac{\partial u_{iz2}}{\partial Z} &= \frac{\partial n_{i1}}{\partial T} + \frac{\partial u_{ix2}}{\partial x} + \frac{\partial u_{iy2}}{\partial y} + \frac{\partial (n_{i1}u_{iz1})}{\partial Z}, \\ \lambda \frac{\partial n_{e2}}{\partial Z} - \frac{\partial u_{ez2}}{\partial Z} &= \frac{\partial n_{e1}}{\partial T} + \frac{\partial (n_{e1}u_{ez1})}{\partial Z}, \\ \lambda \frac{\partial u_{iz2}}{\partial Z} - \frac{\partial \phi_2}{\partial Z} &= \frac{\partial u_{iz1}}{\partial T} + u_{iz1} \frac{\partial u_{iz1}}{\partial Z}, \\ \lambda^2 \frac{\partial n_{e2}}{\partial Z} - \frac{\partial \phi_2}{\partial Z} &= \frac{\lambda^2 (3\alpha_0^2 + 1)}{3(\alpha_0^2 + 1)} n_{e1} \frac{\partial n_{ez1}}{\partial Z} + \delta \lambda^3 u_{ez1} \frac{\partial n_{e1}}{\partial Z} \\ \frac{\partial n_{e2}}{\partial Z} - \frac{\partial n_{i2}}{\partial Z} &= \left(\frac{\partial^3 \phi_1}{\partial Z \partial X^2} + \frac{\partial^3 \phi_1}{\partial Z \partial Y^2} + \frac{\partial^3 \phi_1}{\partial Z^3} \right) + 2\delta \left(u_{iz1} \frac{\partial u_{iz1}}{\partial Z} - u_{ez1} \frac{\partial u_{ez1}}{\partial Z} \right). \end{aligned} \tag{34}$$

Combining these equations, we obtain a partial-differential equation (PDE) in the form:

$$\frac{\partial \phi_1}{\partial T} + A \phi_1 \frac{\partial \phi_1}{\partial Z} + B \frac{\partial^3 \phi_1}{\partial Z^3} + C \left(\frac{\partial^3 \phi_1}{\partial Z \partial X^2} + \frac{\partial^3 \phi_1}{\partial Z \partial Y^2} \right) = 0, \quad (35)$$

where the (real) coefficients A, B and C are given by the expressions:

$$A = \left[\left(1 - \frac{\delta \beta}{2} \right) \alpha_0^2 + \frac{4}{3} \right] / [\beta \alpha_0^2 (\alpha_0^2 + 1)]^{1/2}, \quad (36)$$

$$B = \frac{1}{2} \left(\frac{\beta \alpha_0^2}{\alpha_0^2 + 1} \right)^{3/2}, \quad (37)$$

and

$$C = B (\Omega^{-2} + 1). \quad (38)$$

The latter PDE is recognized as the Zakharov-Kuznetsov (ZK) equation [28].

VI. SOLITARY WAVE ANALYSIS

To study the properties of IA solitary waves propagating in a direction making an angle θ with the z -axis, i.e., with the external static magnetic field, say lying in the ZX plane, we shall first rotate the coordinate axes (X, Z) by an angle θ and making use of the following transformation of the independent variables [31–33]

$$\begin{aligned} \zeta &= X \cos \theta - Z \sin \theta, & \xi &= X \sin \theta + Z \cos \theta, \\ \eta &= Y & \text{and} & \quad \tau = T. \end{aligned} \quad (39)$$

Applying these transformations to the ZK Eq. (35), we obtain

$$\begin{aligned} \frac{\partial \phi_1}{\partial \tau} + S_1 \phi_1 \frac{\partial \phi_1}{\partial \xi} + S_2 \frac{\partial^3 \phi_1}{\partial \xi^3} + S_3 \phi_1 \frac{\partial \phi_1}{\partial \zeta} + S_4 \frac{\partial^3 \phi_1}{\partial \zeta^3} + \\ S_5 \frac{\partial^3 \phi_1}{\partial \xi^2 \partial \zeta} + S_6 \frac{\partial^3 \phi_1}{\partial \xi \partial \zeta^2} + S_7 \frac{\partial^3 \phi_1}{\partial \xi \partial \eta^2} + S_8 \frac{\partial^3 \phi_1}{\partial \zeta \partial \eta^2} = 0, \end{aligned} \quad (40)$$

where

$$\left. \begin{aligned} S_1 &= A \cos \theta, S_2 = B \cos^3 \theta + C \sin^2 \theta \cos \theta, \\ S_3 &= -A \sin \theta, S_4 = -B \sin^3 \theta - C \cos^2 \theta \sin \theta, \\ S_5 &= 2C \left(\sin \theta \cos^2 \theta - \frac{1}{2} \sin^3 \theta \right) - 3B \cos^2 \theta \sin \theta, \\ S_6 &= -2C \left(\sin^2 \theta \cos \theta - \frac{1}{2} \cos^3 \theta \right) + 3B \sin^2 \theta \cos \theta, \\ S_7 &= C \cos \theta, S_8 = -C \sin \theta. \end{aligned} \right\} \quad (41)$$

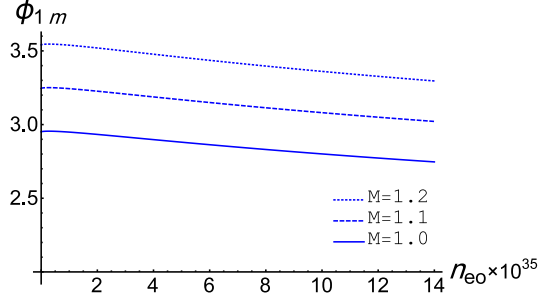


FIG. 7: (Color online) The amplitude of the solitary wave (scaled by φ_0) is depicted versus n_{e0} (in m^{-3}) at different M values. Here, $\theta = 5^\circ$.

Now, we look for a steady state solution of ZK equation in the form

$$\phi_1 = \phi_0(\rho), \quad (42)$$

where $\rho = \xi - M\tau$, and M is the Mach number normalized by the dust acoustic speed c_d . So, the ZK equation in the steady state form leads to,

$$-M \frac{\partial \phi_0}{\partial \rho} + S_1 \phi_0 \frac{\partial \phi_0}{\partial \rho} + S_2 \frac{\partial^3 \phi_0}{\partial \rho^3} = 0. \quad (43)$$

Using the appropriate boundary conditions, namely ϕ_0 and derivatives vanishing as ρ goes to infinity, Eq. (20) has the following solution

$$\phi_0(\rho) = \phi_m \operatorname{sech}^2 \left(\frac{\rho}{W} \right), \quad (44)$$

where ϕ_m and W are the amplitude and the width of the solitary wave, respectively; these are given by the expressions

$$\phi_m = 3M/S_1 \quad \text{and} \quad W = 2\sqrt{S_2/M}. \quad (45)$$

Obviously, reality of the width W imposes $S_2 > 0$. Furthermore, the polarity of the potential pulse, i.e. the sign of the solitary wave function is positive if $S_1 > 0$, and negative otherwise ($S_1 < 0$). Accordingly, the electric field $\vec{\mathbf{E}}$ may be calculated, based on Eq. (44), as

$$\vec{\mathbf{E}} = E_0 \operatorname{sech}^2 \left(\frac{\rho}{W} \right) \tanh \left(\frac{\rho}{W} \right) \begin{pmatrix} \sin \theta \\ 0 \\ \cos \theta \end{pmatrix}, \quad (46)$$

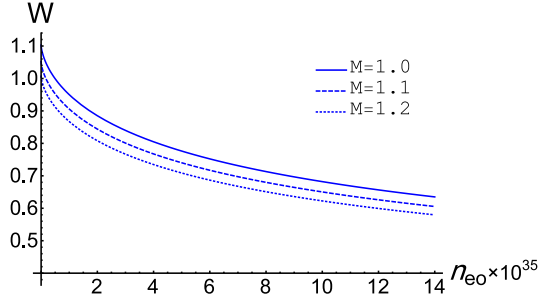


FIG. 8: (Color online) The width of the solitary wave (scaled by L_0) is depicted versus n_{e0} (in m^{-3}) for different M values. Here, $\theta = 5^\circ$, and $\Omega(= \frac{\omega_{ci}}{\omega_{pi}}) = 0.25$.

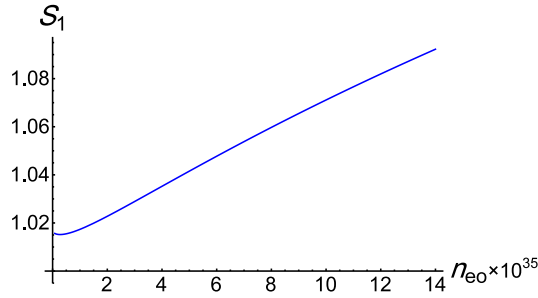


FIG. 9: (Color online) The coefficient S_1 is depicted versus n_{e0} (in m^{-3}). Here, $\theta = 5^\circ$.

in column vector notation, i.e. $\mathbf{v} = v_x \hat{x} + v_y \hat{y} + v_z \hat{z} = (v_x, v_y, v_z)^T$. The maximum electric field reads $E_0 = \frac{3}{S_1} \sqrt{\frac{M^3}{S_2}}$. It is clear from Eqs. (41) and (45) that the amplitude and the width of the solitary wave depend on the electron degeneracy. Figures 7 and 8 show that both amplitude and width of the solitary wave decrease as n_{e0} increases.

The coefficients S_1 and S_2 are depicted in terms of n_{e0} in Figs. 9 and 10. It is found that $S_1(S_2)$ increases (decreases) rapidly as n_{e0} increases.

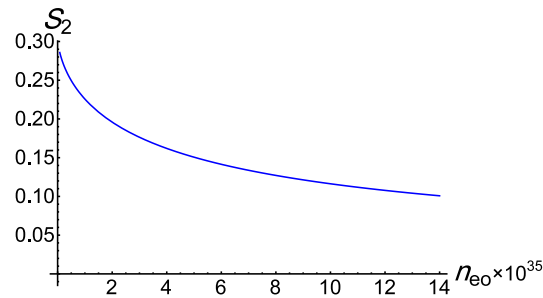


FIG. 10: (Color online) The coefficient S_2 is depicted versus n_{e0} (in m^{-3}). Here, $\theta = 5^\circ$, and $\Omega(= \frac{\omega_{ci}}{\omega_{pi}}) = 0.25$.

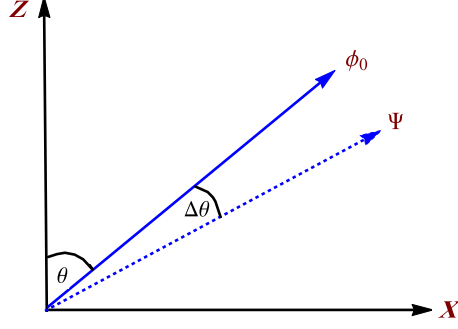


FIG. 11: Geometrical direction diagram of the propagating wave at equilibrium ϕ_0 and the perturbation part Ψ .

VII. STABILITY ANALYSIS

We shall now apply the small- k expansion perturbation method [31, 32] to study the stability of obliquely propagating IA structures. We assume that [33, 34]

$$\phi_1 = \phi_0(\rho) + \Psi(\rho, \zeta, \eta, \tau), \quad (47)$$

where ϕ_0 is defined by Eq.(44) and Ψ represents a long wavelength plane wave perturbation in an oblique direction, given by

$$\Psi(\rho, \zeta, \eta, \tau) = \psi(\rho) e^{i[k(l_\xi \rho + l_\zeta \zeta + l_\eta \eta) - \gamma \tau]}. \quad (48)$$

Obviously, (l_ξ, l_ζ, l_η) are directional cosines, hence $l_\xi^2 + l_\zeta^2 + l_\eta^2 = 1$.

Assuming small values of k , $\psi(\rho)$ and γ can be expanded as

$$\psi(\rho) = \psi_0 + k\psi_1 + k^2\psi_2 + \dots, \quad (49)$$

$$\gamma = k\gamma_1 + k^2\gamma_2 + \dots. \quad (50)$$

Substituting Eq. (47) into Eq. (40) and linearizing with respect to ψ , the linearized ZK equation becomes

$$\begin{aligned} \frac{\partial \Psi}{\partial \tau} - M \frac{\partial \Psi}{\partial \rho} + S_1 \phi_0 \frac{\partial \Psi}{\partial \rho} + S_1 \Psi \frac{\partial \phi_0}{\partial \rho} + S_2 \frac{\partial^3 \Psi}{\partial \rho^3} + \\ S_3 \phi_0 \frac{\partial \Psi}{\partial \zeta} + S_4 \frac{\partial^3 \Psi}{\partial \zeta^3} + S_5 \frac{\partial^3 \Psi}{\partial \rho^2 \partial \zeta} + S_6 \frac{\partial^3 \Psi}{\partial \rho \partial \zeta^2} + \\ S_7 \frac{\partial^3 \Psi}{\partial \rho \partial \eta^2} + S_8 \frac{\partial^3 \Psi}{\partial \zeta \partial \eta^2} = 0. \end{aligned} \quad (51)$$

Substituting Eqs. (48 – 50) into Eq. (51) and equating the coefficients of the same powers of k , in the zeroth-order, we get

$$(-M + S_1\phi_0)\psi_0 + S_2\frac{d^2\psi_0}{d\rho^2} = \tilde{C}, \quad (52)$$

where \tilde{C} is the integration constant. It is clear from Eq (43) that the homogeneous part of this equation has two linearly independent solutions, namely, [33]

$$f = \frac{d\phi_0}{d\rho}, \quad g = f \int^\rho \frac{d\rho}{f^2}. \quad (53)$$

Therefore, the general solution of this zeroth-order, Eq. (52), can be written as

$$\psi_0 = C_1f + C_2g - \tilde{C}f \int^\rho \frac{g}{\tilde{W}}d\rho + \tilde{C}g \int^\rho \frac{f}{\tilde{W}}d\rho, \quad (54)$$

where C_1 and C_2 are the integration constants and \tilde{W} is the Wronskian defined by $\tilde{W} = f(dg/d\rho) - g(df/d\rho)$. Evaluating all integrals, the general solution of the zeroth order equation, assuming finite ψ_0 as $\rho \rightarrow \pm\infty$, can be finally simplified to

$$\psi_0 = C_1f. \quad (55)$$

The first-order equation, obtained from Eqs (48 – 51) and (55) can be expressed, after integration, as

$$\begin{aligned} &(-M + S_1\phi_0)\psi_1 + S_2\frac{d^2\psi_1}{d\rho^2} = \\ &iC_1 \left[\beta_1 \tanh^2\left(\frac{\rho}{W}\right) + \beta_2 \right] \phi_0 + C_3, \end{aligned} \quad (56)$$

where C_3 is another integration constant and β_1 and β_2 are given by

$$\beta_1 = \frac{1}{2}\phi_m\mu_1 - \frac{6}{W^2}\mu_2, \quad (57)$$

$$\beta_2 = \gamma_1 + Ml_\xi - \frac{1}{2}\phi_m\mu_1 + \frac{2}{W^2}\mu_2, \quad (58)$$

where

$$\mu_1 = (S_1l_\xi + S_3l_\zeta) \quad \text{and} \quad \mu_2 = (3S_2l_\xi + S_5l_\zeta). \quad (59)$$

Similarly, the general solution of the first order equation, assuming finite ψ_1 as $\rho \rightarrow \pm\infty$, is given by

$$\psi_1 = K_1f + \frac{iC_1W^2}{8S_2} \left[(\beta_1 + \beta_2)\rho f + 2\left(\frac{1}{3}\beta_1 + \beta_2\right)\phi_0 \right], \quad (60)$$

where K_1 is an arbitrary constant. The second order equation, obtained from Eq (51), is given as

$$\left(-M\frac{d}{d\rho} + S_1\frac{d}{d\rho}\phi_0 + S_2\frac{d^3}{d\rho^3}\right)\psi_2 = Q, \quad (61)$$

where

$$Q = i\gamma_2\psi_0 + i(\gamma_1 + Ml_\xi - \mu_1\phi_0)\psi_1 + \mu_3\frac{d\psi_0}{d\rho} - i\mu_2\frac{d^2\psi_1}{d\rho^2}, \quad (62)$$

$$\mu_3 = (3S_2l_\xi^2 + 2S_5l_\zeta l_\xi + S_6l_\zeta^2 + S_7l_\eta^2), \quad (63)$$

The existence of the solution of Eq (61) requires that Q must be orthogonal to the kernel of the adjoint operator to the operator L , which is given by

$$L = -M\frac{d}{d\rho} + S_1\frac{d}{d\rho}\phi_0 + S_2\frac{d^3}{d\rho^3}. \quad (64)$$

Thus, we obtain the following consistency condition

$$\int_{-\infty}^{\infty} \phi_0 Q d\rho = 0. \quad (65)$$

Substituting for ψ_0 and ψ_1 from Eqs. (55) and (60), respectively, into Eq. (65), we obtain the following dispersion relation

$$\gamma_1 = \Delta - Ml_\xi + \sqrt{\Delta^2 - \Gamma}, \quad (66)$$

where

$$\Delta = \frac{2}{3}(\mu_1\phi_m - 2\mu_2/W^2), \quad (67)$$

$$\Gamma = \frac{16}{45}(\mu_1^2\phi_m^2 - 3\mu_1\mu_2\phi_m/W^2 - 3\mu_2^2/W^4 + 12S_2\mu_3/W^4). \quad (68)$$

Hence, from Eq. (66), we notice that instability occurs if the following condition is satisfied:

$$\Gamma - \Delta^2 > 0, \quad (69)$$

Thus, using Eqs. (41, 45, 59, 63, 67 – 68), we obtain the growth rate $g_r = \sqrt{\Gamma - \Delta^2}$ of the instability as follows

$$g_r = \frac{2M}{\sqrt{15}} \frac{(\Omega^2 + 1)^{1/2} I_{cr}^{1/2}}{(\Omega^2 + 1) \cos \theta - \cos^3 \theta}. \quad (70)$$

We retain the instability criterion $I_{cr} > 0$, where

$$I_{cr} = \frac{1}{6}l_\zeta^2(-2\Omega^2 - 5 + (8\Omega^2 + 5)\cos 2\theta) + 2l_\eta^2 \frac{((\Omega^2 + 1)\cos \theta - \cos^3 \theta)^2}{2\Omega^2 + 1 - \cos 2\theta}, \quad (71)$$

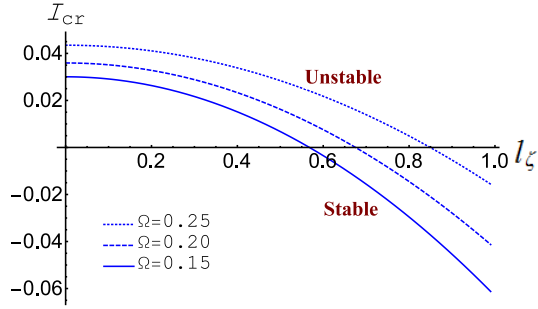


FIG. 12: The characteristic function I_{cr} , given by (71), is depicted versus the direction cosine l_ζ (cf. Eq (49)), for different Ω values. Here, $l_\eta = 0.6$, $\theta = 15^\circ$ and $M = 1.2$.

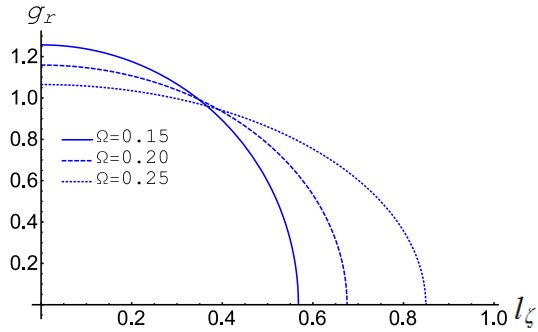


FIG. 13: The instability growth rate g_r , given by (70), is depicted versus the direction cosine l_ζ (cf. Eq. (48)), for different Ω values. Here, $l_\eta = 0.6$, $\theta = 15^\circ$ and $M = 1.2$.

It is clear from Eq. (70) for g_r that the instability growth rate depends on Ω ($= \omega_{ci}/\omega_{pi}$), which is affected by the electron degeneracy at equilibrium (via the dependence of ω_{pi} on the equilibrium density), assuming that a constant external magnetic field is considered. Figure 12 determines the parametric region of instability, $I_{cr} > 0$, with respect to l_ζ and Ω . Here, the points at which $I_{cr} = 0$ are the transient points from instability to stability. Also, the growth rate of instability g_r decreases rapidly as the direction cosine l_ζ increases and g_r is drastically affected by variations in Ω values, as shown in Fig. 13.

VIII. CONCLUSIONS

We have employed a quantum hydrodynamic model for a magnetized relativistic degenerate plasma, in order to investigate the propagation of linear and nonlinear electrostatic solitary waves of electrostatic nature and to characterize their dispersion properties.

A set of modified expressions have been presented for the characteristic charge screening length, λ_{sc}^{rel} , and for the sound speed in the plasma, C_s^{rel} , taking into account the relativistic corrections. The sound speed C_s^{rel} decreases rapidly as n_{e0} increases. Inversely, λ_{sc}^{rel} increases with higher n_{e0} , as shown in Figs. 5 and 6.

A nonlinear perturbation technique was employed to study nonlinear small-amplitude weakly superacoustic ion-acoustic excitations. A Zakharov-Kuznetsov (ZK) type equation was derived and a family of exact solutions was analytically obtained. These represent solitary wave type structures in the form of pulses, whose amplitude and width decrease as n_{e0} increases (see Fig. 7 and 8). A (3D) instability analysis for the nonlinear supersonic pulses, adopting a small $-k$ expansion methodology, has revealed that these structures are unstable. Analytical expressions for the instability growth rate g_r have been deduced.

Our model may be useful in understanding the dynamics of collective excitations in metallic nanostructures and thin films [4], and also the physics of quantum diodes [5], nanophotonics and nanowires [6], nanoplasmonics [7], high-gain quantum free-electron lasers [8], quantum wells and piezomagnetic quantum dots [9]. Degenerate plasmas may also exist in dense astrophysical objects, e.g. in the core of giant planets [10] and in the crust of white dwarfs, brown dwarfs, neutron stars, and magnetars [11, 12]. As discussed above, the existence of electrostatic modes such environments has been suggested in the past [19, 19–22], and yet, not surprisingly (given the obvious intrinsic observation and diagnostics issues involved), these haven't been observed to date [20].

Acknowledgments

EEB acknowledges financial support from the Cultural Affairs and Missions Sector, Egyptian Ministry of Higher Education during his research visit to Queen's University Belfast, Belfast, UK. FH and IK gratefully acknowledge support from the Brazilian research fund CNPq (Conselho Nacional de Desenvolvimento Científico e Tecnológico-Brasil), as well as from the European Union (EU) FP7 IRSES Programme (grant 612506, QUANTUM PLAS-

* Electronic address: eebebery@gmail.com; The author to whom correspondence should be addressed.

† Electronic address: fernando.haas@ufrgs.br; <http://professor.ufrgs.br/fernando-haas/>

‡ Electronic address: IoannisKourakisSci@gmail.com; www.kourakis.eu

- [1] J. Lindl, *Phys. Plasmas* **2**, 3933 (1995).
- [2] S. H. Glenzer, O. L. Landen, P. Neumayer, R. W. Lee, K. Widmann, S. W. Pollaine, R. J. Wallace, G. Gregori, A. Hill, T. Bornath, R. Thiele, V. Schwarz, W.-D. Kraeft, and R. Redmer, *Phys. Rev. Lett.* **98**, 065002 (2007).
- [3] P. Neumayer, C. Fortmann, T. Dppner, P. Davis, R. W. Falcone, A. L. Kritcher, O. L. Landen, H. J. Lee, R. W. Lee, C. Niemann, S. Le Pape, and S. H. Glenzer, *Phys. Rev. Lett.* **105**, 075003 (2010).
- [4] N. Crouseilles, P. A. Hervieux, and G. Manfredi, *Phys. Rev. B* **78**, 155412 (2008).
- [5] L. K. Ang, T. J. T. Kwan, and Y. Y. Lau, *Phys. Rev. Lett.* **91**, 208303 (2003).
- [6] W. Barnes, A. Dereux, and T. Ebbesen, *Nature (London)* **424**, 824 (2003).
- [7] E. Ozbay, *Science* **311**, 189 (2006).
- [8] A. Serbeto, L. F. Monteiro, K. H. Tsui, and J. T. Mendonc, *Plasma Phys. Controlled Fusion* **51**, 124024 (2009).
- [9] R. M. Abolfath, A. G. Petukhov, and I. utic, *Phys. Rev. Lett.* **101**, 207202 (2008).
- [10] H. M. Horn, *Science* **252**, 384 (1991).
- [11] T. Guillot, *Science* **286**, 72 (1999).
- [12] D. Koester and G. Chanmugam, *Rep. Prog. Phys.* **53**, 837 (1990).
- [13] S. Chandrasekhar, *Philos. Mag.* **11**, 592 (1931).
- [14] S. Chandrasekhar, *Mon. Not. R. Astron. Soc.* **95**, 207 (1935).
- [15] P. K. Shukla, B. Eliasson, *Phys. Usp.* **53**, 51 (2010).
- [16] P. K. Shukla and B. Eliasson, *Rev. Mod. Phys.* **83**, 885 (2011).
- [17] F. Haas and I. Kourakis, *Plasma Phys. Control. Fusion* **57**, 044006 (2015).
- [18] M. Mc Kerr, F. Haas, I. Kourakis, *Phys. Rev. E*, **90**, 033112 (2014).

- [19] B. Eliasson and P. K. Shukla, *Europhys. Lett.* **97**, 15001 (2012).
- [20] R. Silvotti, G. Fontaine, M. Pavlov *et al.*, *Astron. Astrophys.* **525**, A64 (2011).
- [21] J. P. Ostriker, *Ann. Rev. Astron. Astrophys.* **9**, 353 (1971).
- [22] V. E. Fortov, *Phys. Usp.* **52**, 615 (2009).
- [23] M. Marklund, B. Eliasson and P. K. Shukla, *Phys. Rev. E* **76**, 067401 (2007).
- [24] H. Tercas, J. T. Mendonca and P. K. Shukla, *Phys. Plasmas* **15**, 072109 (2008).
- [25] W. F. El-Taibany and A. A. Mamun, *Phys. Rev. E* **85**, 026406 (2012).
- [26] M. McKerr, I. Kourakis and F. Haas, *Plasma Phys. Contrroll. Fusion* **56**, 035007 (2014).
- [27] V. E. Zakharov and E. A. Kuznetsov, *Sov. Phys. JETP* **39**, 285 (1974).
- [28] *Nonlinear Waves, Solitons and Chaos*, Eryk Infeld and George Rowlands, 2nd Edition (Cambridge University Press, 2000).
- [29] D.J. Korteweg and G. de Vries, *Phil. Mag. Series 5*, **39:240**, 422 (1895).
- [30] P. Frycz and E. Infeld, *J. Plasma Phys.* **41**, 441 (1989).
- [31] M. A. Allen and G. Rowlands, *J. Plasma Phys.* **50**, 413 (1993).
- [32] M. A. Allen and G. Rowlands, *J. Plasma Phys.* **53**, 63 (1995).
- [33] A. A. Mamun, *Phys. Scr.* **58**, 505 (1998).
- [34] S. K. El-Labany, W. F. El-Taibany, and E. E. Behery, *Phys. Rev. E* **88**, 023108 (2013).
- [35] M. F. Bashir, E. E. Behery, and W. F. El-Taibany, *Phys. Plasmas* **22**, 062112 (2015).
- [36] F. Haas and B. Eliasson, *Phys. Scripta* **90**, 088005 (2015).
- [37] H. Washimi and T. Taniuti, *Phys. Rev. Lett.* **17**, 996 (1966).